IEEE Access
Multidisciplinary | Rapid Review | Open Access Journal

Received December 29, 2021, accepted January 17, 2022, date of publication January 20, 2022, date of current version February 14, 2022.

Digital Object Identifier 10.1109/ACCESS.2022.3144979

Performance Analysis of Multiple Antennas Synthetic False Target Jamming

YUHANG NING AND MENGXIA YU
School of Physics, University of Electronic Science and Technology of China, Chengdu 610056, China
Corresponding author: Mengxia Yu (yumengxia@uestc.edu.cn)

ABSTRACT The radar jamming technology has been studied in this paper mainly, which uses the antenna synthetic wave to generate phase distortion at the signal reception to carry out angle measuring jamming, such as traditional cross-eye jamming. However, cross-eye jamming has strict parameter tolerance. To improve the tolerance range of the phase parameters, a multiple antennas synthetic false target electromagnetic jamming technique is proposed in this paper, which has a wider phase parameter tolerance and jamming range. The jamming method can be regarded as an improved cross eye jamming method. We can conclude that this method can generate a ''false target'' in space and far away from the carrier which has jamming system, which mislead the radar to point to ''false target'' rather than to real targets. A jamming system with three jamming antennas was considered as the research object. The position of ''false target'' can be controlled casually by adjusting the feed amplitude and phase of the three antennas simultaneously. The jamming mathematical model of synthetic false target with three antenna emitters is constructed under the sum and difference channel transceiver mechanism of radar in this paper. The error angle and synthetic gain of the three jamming antennas were derived. The phase parameter tolerance of the proposed method was obtained- and compared with cross-eye jamming. A rigorous mathematical derivation is proposed in this paper, and the superiority of the multiple antennas synthetic false target jamming method is verified.

INDEX TERMS Antenna, jamming, radar, tolerance analysis.

I. INTRODUCTION

The angle-measurement deception jamming method was investigated, and we found that cross-eye jamming is an angle-measurement jamming method based on the principle of angular scintillation [1], [2]; Which uses two antennas fed with the same amplitude but a phase difference of 180° The principle of cross-eye jamming is that two signals produce wavefront phase distortion at the receiving terminal, which offsets the normal direction of the radar angle measurement. At this time, the radar still searches according to the normal direction of the wavefront, and then deviates from the true target direction, resulting angle measurement error [3], [4]. The mechanism of cross-eye jamming determines that the successful implementation of interference has strict tolerance of antenna feed phase parameters. In practice, perfect feed information is too harsh for hardware. The antenna platform of the cross-eye is sensitive to the rotation angle. Subsequently, improved cross-eye jamming such as reverse cross-eye and multi-source reverse cross-eye have been developed, and disadvantages such as harsh parameter tolerance and low degrees of freedom have been improved [5]–[9]. In 2010, W. Du Plessis [12] conducted a rigorous theoretical analysis and mathematical model derivation of the two-point source reverse cross-eye jamming model. A general conclusion of the two-source reverse cross-eye jamming is formed. The introduction of the reverse antenna structure eliminates the phase difference between the two interference signals caused by the path difference, and reduces the hardware requirements compared to the traditional cross-eye. However, cross-eye jamming from two point sources still faces the problem of low degrees of freedom. From 2011 to 2012, Du Plessis [5], [10], [11] continued the parameter tolerance and platform echo analyses of the previously proposed reverse cross-eye. The results show that the larger the angle factor of the cross-eye jamming, the more severe the tolerance of the amplitude and phase parameters. Therefore, it is necessary to improve the parameter tolerance of the two-point source reverse cross-eye. From 2016 to 2019, Du Plessis [9], [13], and [14] proposed a multi-loop reverse cross eye interference model.

The associate editor coordinating the review of this manuscript and approving it for publication was Ladislau Matekovits.

Adding a reverse cross-eye loop and controlling each loop to have the same phase center proves that the multi-jamming loop cross-eye with a high degree of freedom is helpful in improving the interference angle of traditional cross-eye jamming. An increase in the number of interference loops is helpful for improving the parameter tolerance of cross-eye interference for the same angle factor. However, it also points out that the improvement of the interference effect is at the cost of increasing the system complexity, and the difference between interference loops will worsen the interference effect of the multi-source reverse cross-eye. In the worst case, the interference system makes the carrier beacon machine. In 2019, Du Plessis [15] proposed two methods for static and dynamic compensation of loop differences between different loops in a multi-loop reverse cross-eye. In 2020, Du Plessis [16] proposed a cross-eye jammer based on a phase-conjugating (PC) retrodirective array. Such PC cross-eye jammers eliminate the delay inherent in traditional Van Atta (VA) cross-eye jammers and induce errors in radars that use the same antenna beam for transmission and reception, whereas VA cross-eye jammers do not. Validated simulations were performed to confirm the effectiveness and retrodirective properties of the PC cross-eye jammers. In 2020, Liu *et al.* [17] proposed a novel four-point source reverse cross eye interference technique based on direction of arrival (DOA). The antenna layout of the interference loop was optimized using DOA information, and the influence of the amplitude and phase parameters on the cross-eye jamming effect was analyzed. The results show that this method is superior to traditional and orthogonal four-point source reverse cross eye interference technology in terms of the interference effect and parameter tolerance. In 2020, Kim *et al.* [18] proposed a phased-array reverse cross-eye interference structure composed of a multi-channel phased-array antenna based on two-source reverse cross-eye jamming. The multichannel characteristics of phased arrays increase the freedom of the system channel matching. The implementation and testing of a retrodirective cross-eye jammer against a phase-comparison radar was described in 2021 by Pieterse and Du Plessis [19]. Both the radar and jammer were implemented using software-defined ratios (SDRs) and power dividers. Calibration of the cross-eye jammer based on minimization of the sum channel radar return is described. The presented results show that the system is a true retrodirective cross-eye jammer and that cross-eye jamming can indeed induce large angular errors in radar, with conditions corresponding to a break-lock condition being achieved. This represents the latest progress in the study of cross-eye interference. However, the focus of these studies is to repair some defects of the cross-eye using methods or to verify the effectiveness of cross-eye interference by other means. However, the tolerance of strict phase parameters has not been solved well by current cross-eye studies.

To ameliorate the strict phase parameter tolerance performance of existing interference technology when a jamming system is applied. A false target electromagnetic interference method based on multiple antennas synthetic is proposed in this paper. Three antennas were used as the basic model for the theoretical research. A false target can be generated in space when three radiation elements in the array antennas radiate the same frequency signals simultaneously. The position of the composite center angle can be changed when the feed amplitude and phase of each emitter are adjusted to simulate the real target echo information. False target electromagnetic interference was successfully realized on the two-dimensional plane instead of the one-dimensional interference of the cross-eye. Multiple-antenna synthetic jamming can effectively improve the performance of harsh phase parameter tolerance. Further research will be conducted in this paper. Multiple antenna synthetic false target technology has been proposed, which combines the sum and difference channel transceiver principle of radar. The echo signal and jamming signal received by radar antenna beams are analyzed, a scientific mathematical model of the jamming error angle for multiple antennas jamming is established; The tolerance range of multi antenna interference phase parameters is analyzed. It is proven that the false target position has been controlled effectively by adjusting multiple antenna feed parameters, and the superiority of the proposed method in terms of phase parameter tolerance to cross-eye jamming has been proven.

II. BASIC THEORY OF RADAR AMPLITUDE AND PHASE COMPARISON ANGLE MEASUREMENT

A. THE FIRST ANGLE MEASUREMENT METHOD, AMPLITUDE- COMPARISON

The basic theory of the two different angle measurement methods of radar was introduced before introducing the jamming method we proposed in detail. Radar angle measurement methods can be divided into amplitude and phase-comparison angle measurement methods [12], [20]–[22].

In the amplitude-comparison angular method, two (or multiple) partially overlapping beams receive the echo signal simultaneously and then process the sum and difference channels according to the returns received by the two beams. The two echo signals have different amplitudes and equal phases. The sum channel signal is obtained by adding process, and the difference channel signal is obtained by subtracting process. Therefore, the sum channel signal amplitude is the sum of the two echo signal amplitudes, which has nothing to do with the angle at which the target deviates from the radar Los. The amplitude of the difference channel signal is the difference between the amplitudes of the two echo signals; the size of the value represents the angle of the target from the radar Los, and the positive and negative symbols represent the direction of the target from the radar Los. Angular information can be obtained by normalizing the two-channel signals.

The specific basic theoretical part will be described below.

Basic information is shown in Fig.1(a). The two radar beam pattern functions are obtained as follows. $F(\theta)$ is a radar-antenna pattern [22].

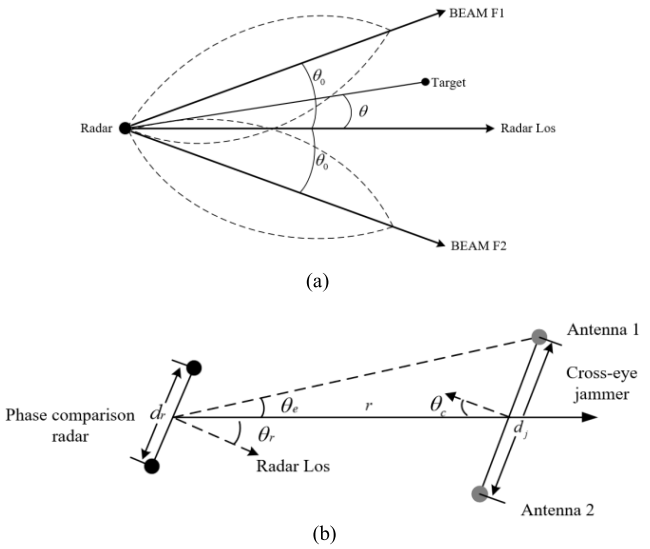

FIGURE 1. Schematic diagram of amplitude comparison radar (a); Jamming scene of cross eye system to phase comparison radar (b).

Then

$$F_1(\theta) = F(\theta_0 + \theta)$$
$$F_2(\theta) = F(\theta_0 - \theta) \tag{1}$$

Two radar beams will receive the signals like that

$$\mu_1(\theta) = KF(\theta_0 + \theta)$$
$$\mu_2(\theta) = KF(\theta_0 - \theta) \tag{2}$$

where K is the echo amplitude coefficient, and the sum and difference channel signals of the two beams can be obtained as:

$$\mu_\Sigma(\theta) = \mu_1(\theta) + \mu_2(\theta) = K(F(\theta_0 + \theta) + F(\theta_0 - \theta))$$
$$\mu_\Delta(\theta) = \mu_1(\theta) - \mu_2(\theta) = K(F(\theta_0 + \theta) - F(\theta_0 - \theta)) \tag{3}$$

The results of the next step can be obtained by Taylor expansion.

$$F(\theta_0 + \theta) = F(\theta_0) + F(\theta_0)'\theta + o(\theta^2)$$
$$F(\theta_0 - \theta) = F(\theta_0) - F(\theta_0)'\theta + o(\theta^2) \tag{4}$$

Ignoring minimum value and normalizing the sum and difference channel signals. And the target angle measurement information can be obtained by amplitude comparison method. The results can be obtained by combined (3) and (4).

$$\frac{\mu_\Delta(\theta)}{\mu_\Sigma(\theta)} = \frac{F(\theta_0)'}{F(\theta_0)}\theta = \mu\theta \tag{5}$$
$$\theta = \frac{1}{\mu}\frac{\mu_\Delta(\theta)}{\mu_\Sigma(\theta)} \tag{6}$$

where μ is the normalized slope of the radar antenna pattern on θ_0 and θ is the angle offset from the radar LOS.

B. THE SECOND ANGLE MEASUREMENT METHOD, PHASE- COMPARISON

Here, is the second angle measurement method. The phase comparison angle measurement radar sum channel and difference channel were used to receive the echoes. The difference channel was normalized to the sum channel echoes to obtain the error angle signal [12], [21].

An example is the cross-eye system jam phase comparison angle-measuring radar shown in Fig.1 (b). The black dot represents the receiving radar and the grey dot represents the jammer. Two antennas exist in a jamming system. One is the top antenna and the other is the bottom antenna. The angular information is shown in Fig.1(b). According to [12], the gain of the sum and difference channel of the phase comparison radar in the direction of the top and bottom jamming antennas can be written as follows:

$$S_{1,2} = \cos\left[\beta\frac{d_r}{2}\sin(\theta_r \pm \theta_e)\right]P_r(\theta_r \pm \theta_e)$$
$$D_{1,2} = j\sin\left[\beta\frac{d_r}{2}\sin(\theta_r \pm \theta_e)\right]P_r(\theta_r \pm \theta_e) \tag{7}$$

where S_i and $D_i(i = 1, 2)$ represent the sum and difference in channel gains in the direction of the nth jamming antenna, respectively (1 represents the top antenna and 2 represents the bottom antenna). Then the sum channel signal S_J and difference channel signal D_J signal received by the radar are obtained, as in reference [12].

$$M_J = \Im\left(\frac{D_J}{S_J}\right) \to \theta \tag{8}$$

where $\Im$ denotes the imaginary part. The sum channel and difference channel received signal by the radar will be used calculate the angle information. The angle signals θ will be obtained by deducing M_J (In order to make the article more concise, arrow symbols are used instead of derivation process). More accurate and detailed process has been proposed in [12].

The following section presents the theoretical modeling and mathematical derivation of the multi antenna synthetic false target interference proposed in this paper.

III. MULTIPLE ANTENNA SYNTHETIC FALSE TARGET MATHEMATICAL MODEL

A. THE FIRST ERROR ANGLE DERIVATION METHOD, AMPLITUDE

A mathematical model was established using two different methods of angle measurement. The jamming scene for the first method is shown in Fig.2(a). where a_1, a_2, a_3 is the jamming antenna. T represents the center position of the jamming platform plane. The radar- receiving beams were F1, F2, F3, and F4. The beams are symmetrically distributed about the radar LOS axis and partially overlap. The signals received by the four radar beams are denoted as E1, E2, E3, and E4. A more detailed image of the jamming radar scene is shown in Fig.2(b). It is worth mentioning that the three

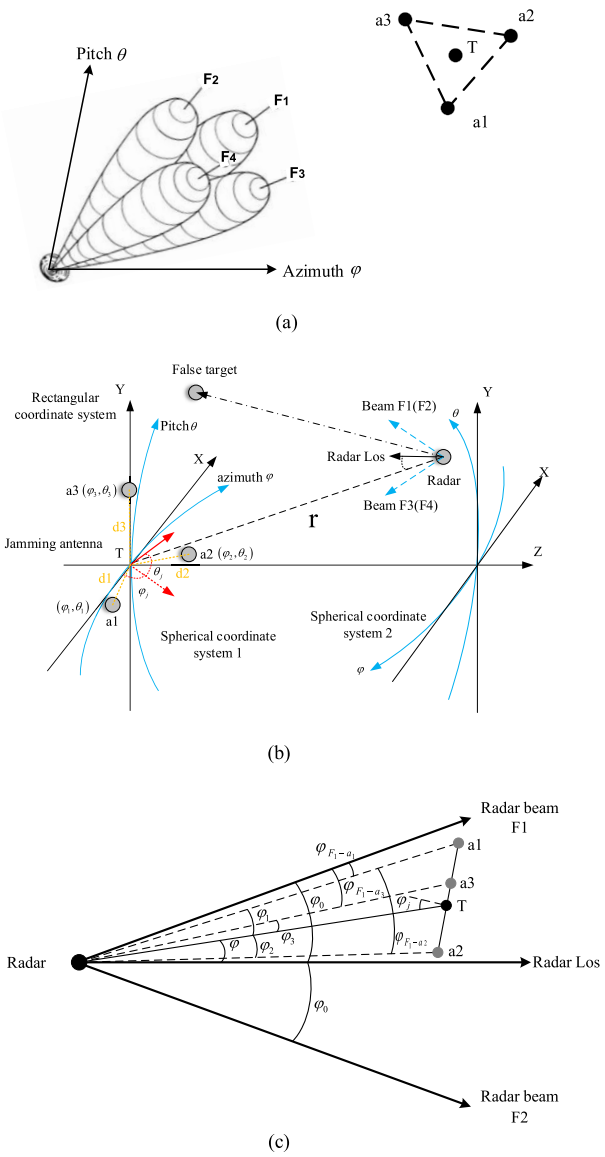

FIGURE 2. Illustration of four radar beams and three jamming antennas (a) Jamming scene of three antennas to the radar (b). Relationship between the jamming antenna and F1and F2 azimuths of the radar beam (c).

jamming antennas are at different baselines. For example, antenna a_3 is not on the same baseline as antenna a_1, a_2.

The coordinates of a_1, a_2, a_3 are $(\varphi_1, \theta_1), (\varphi_2, \theta_2), (\varphi_3, \theta_3)$, which has only two elements in this jamming scene. It is defined as $\varphi_i = d_i/r$; $\theta_i = d_i/r$, whose dimension is rad. The variable $d_i (i = 1, 2, 3)$ is the distance between the jamming antenna $a_i (i = 1, 2, 3)$ and T, which is marked in Fig.2(b). r represents the jamming distance. Taking azimuth as an example, a more detailed explanation of the angular relationship is proposed in Fig.2(c). The angle between the direction of the main lobe of the radar beam and radar LOS is (φ_0, θ_0). The plane angle of the jamming antenna is (φ_j, θ_j). All the information on the relationship between the angles can be provided as follows:

The relationship of Azimuth angle between radar beam F1 and jamming a_1, a_2, a_3 can be obtained.

$$\begin{cases} \varphi_{F_1-a_1} = \varphi_0 - \varphi - \varphi_1 \\ \varphi_{F_1-a_2} = \varphi_0 - \varphi + \varphi_2 \\ \varphi_{F_1-a_3} = \varphi_0 - \varphi - \varphi_3 \end{cases} \tag{9}$$

Similarly, the relationship of the azimuth angle between radar beam F2 and jamming a_1, a_2, a_3 can be obtained.

$$\begin{cases} \varphi_{F_2-a_1} = \varphi_0 + \varphi + \varphi_1 \\ \varphi_{F_2-a_2} = \varphi_0 + \varphi - \varphi_2 \\ \varphi_{F_2-a_3} = \varphi_0 + \varphi + \varphi_3 \end{cases} \tag{10}$$

Equation (9) and (10) can be obtained by observing thee geometric relationship in Fig.2(c), which can be used to write the following formula.

Similarly, all angular relations in Fig.2(b) can be obtained after expansion. The relationship between the radar beam and jamming antenna angle is analyzed as follows. When the jamming system faces the receiving radar, the jamming system conducts angle measurement jamming on the receiving radar, in which the four beams of one pulse of the receiving radar receive a signal. This signal contains the jamming information applied by the jamming system, and the four signals are E1, E2, E3, and E4, respectively. Each radar beam receives its own signal from three jamming antennas; therefore, the signal obtained by the radar beam can be written as three items. The received signals E1, E2, E3, and E4 of the four radar beams can be expressed as (to ensure the formula has a clearer meaning, we use more specific indexes (15) to replace the conclusions of (9) and (10)).

$$\begin{aligned} E_1 = {} & e_1 F_r\left(\varphi_{p1} - \varphi_1, \theta_{p1} + \theta_1\right) + e_2 F_r\left(\varphi_{p1} + \varphi_2, \theta_{p1} + \theta_2\right) \\ & + e_3 F_r\left(\varphi_{p1} - \varphi_3, \theta_{p1} - \theta_3\right) \end{aligned} \tag{11}$$

$$\begin{aligned} E_2 = {} & e_1 F_r\left(\varphi_{p2} + \varphi_1, \theta_{p1} + \theta_1\right) + e_2 F_r\left(\varphi_{p2} - \varphi_2, \theta_{p1} + \theta_2\right) \\ & + e_3 F_r\left(\varphi_{p2} + \varphi_3, \theta_{p1} - \theta_3\right) \end{aligned} \tag{12}$$

$$\begin{aligned} E_3 = {} & e_1 F_r\left(\varphi_{p1} - \varphi_1, \theta_{p2} - \theta_1\right) + e_2 F_r\left(\varphi_{p1} + \varphi_2, \theta_{p2} - \theta_2\right) \\ & + e_3 F_r\left(\varphi_{p1} - \varphi_3, \theta_{p2} + \theta_3\right) \end{aligned} \tag{13}$$

$$\begin{aligned} E_4 = {} & e_1 F_r\left(\varphi_{p2} + \varphi_1, \theta_{p2} - \theta_1\right) + e_2 F_r\left(\varphi_{p2} - \varphi_2, \theta_{p2} - \theta_2\right) \\ & + e_3 F_r\left(\varphi_{p2} + \varphi_3, \theta_{p2} + \theta_3\right) \end{aligned} \tag{14}$$

where

$$\begin{cases} e_1 = A_1 F_r(\varphi, \theta) F_j\left(\varphi_j - \varphi_1, \theta_j + \theta_1\right) e^{j\omega t} \\ e_2 = A_2 F_r(\varphi, \theta) F_j\left(\varphi_j + \varphi_2, \theta_j + \theta_2\right) e^{j(\omega t + \delta_{12})} \\ e_3 = A_3 F_r(\varphi, \theta) F_j\left(\varphi_j - \varphi_3, \theta_j - \theta_3\right) e^{j(\omega t + \delta_{13})} \\ \varphi_{p1} = \varphi_0 - \varphi, \quad \theta_{p1} = \theta_0 - \theta, \quad \theta_{p2} = \theta_0 + \theta, \\ \varphi_{p2} = \varphi_0 + \varphi, \end{cases} \tag{15}$$

e_i are indexes that have no special meaning, where $A_i, i = (1, 2, 3)$ is the feed amplitude of the jamming antennas, $F_r(\varphi, \theta)$ is the radar antenna beam function, $F_r(\varphi_0 - \varphi_1 + \varphi, \theta_0 + \theta_1 - \theta)$ is the radar antenna receive beam function, e^{jwz}, $e^{j(wz+\delta 12)}$, $e^{j(wz+\delta 13)}$ is the time harmonic function of jamming antennas at radar receiver, and $F_j(\varphi, \theta)$

is the jamming antenna beam function. The formula above explains the digital expression of the signal received by the four beams of the radar receiver. The jamming antenna starts jamming only when the detection radar continuously transmits the detection signal and is approaching or already approaching jamming platform, φ and θ is very small when interference is applied. Because the jamming distance is far greater than the distance between the jamming antenna and center T, then $\varphi_1, \theta_1, \varphi_2, \theta_2, \varphi_3, \theta_3$ and $\varphi_1', \varphi_2', \varphi_3', \theta_1', \theta_2', \theta_3'$ can be ignored. We expand and simplify the derivation of (11), (12), (13), and (14) according to the binary Taylor expansion formula (16). The results were as follows.

$$\begin{aligned} &F_r\left(\varphi_0 \pm \varphi_n', \theta_0 \pm \theta_m'\right) \\ &= F_r\left(\varphi_0, \theta_0\right) \pm \varphi_n' F_{r\varphi}\left(\varphi_0, \theta_0\right) \\ &\quad \pm \theta_m' F_{r\theta}\left(\varphi_0, \theta_0\right) + o\left(\varphi_0^2, \theta_0^2\right) \end{aligned} \tag{16}$$

In the all of the formulas, $F_{r\varphi}, F_{r\theta}$ are the first derivative of F_r that based on φ and θ; δ_{12} and δ_{13} are the phase difference of jamming antennas a_2 and a_3 relative to a_1. Combining the above prerequisites and ignoring the minimum, E1, E2, E3, and E4 can be further obtained as

$$\begin{aligned} E_1 &= e_1\left[F_r - \varphi_1' F_{r\varphi} + \theta_1' F_{r\theta}\right] + e_2\left[F_r + \varphi_2' F_{r\varphi} + \theta_2' F_{r\theta}\right] \\ &\quad + e_3\left[F_r - \varphi_3' F_{r\varphi} - \theta_3' F_{r\theta}\right] \end{aligned} \tag{17}$$

$$\begin{aligned} E_2 &= e_1\left[F_r + \varphi_1' F_{r\varphi} + \theta_1' F_{r\theta}\right] + e_2\left[F_r - \varphi_2' F_{r\varphi} + \theta_2' F_{r\theta}\right] \\ &\quad + e_3\left[F_r + \varphi_3' F_{r\varphi} - \theta_3' F_{r\theta}\right] \end{aligned} \tag{18}$$

$$\begin{aligned} E_3 &= e_1\left[F_r - \varphi_1' F_{r\varphi} - \theta_1' F_{r\theta}\right] + e_2\left[F_r + \varphi_2' F_{r\varphi} - \theta_2' F_{r\theta}\right] \\ &\quad + e_3\left[F_r - \varphi_3' F_{r\varphi} + \theta_3' F_{r\theta}\right] \end{aligned} \tag{19}$$

$$\begin{aligned} E_4 &= e_1\left[F_r + \varphi_1' F_{r\varphi} - \theta_1' F_{r\theta}\right] + e_2\left[F_r - \varphi_2' F_{r\varphi} - \theta_2' F_{r\theta}\right] \\ &\quad + e_3\left[F_r + \varphi_3' F_{r\varphi} + \theta_3' F_{r\theta}\right] \end{aligned} \tag{20}$$

where

$$\begin{cases} \varphi_1' = \varphi_1 + \varphi, & \varphi_2' = \varphi_2 - \varphi, \ \varphi_3' = \varphi_3 + \varphi \\ \theta_1' = \theta_1 - \theta, & \theta_2' = \theta_2 - \theta, \ \theta_3' = \theta_3 + \theta \end{cases} \tag{21}$$

$F_r, F_{r\varphi}$ and $F_{r\theta}$ are $F_r\left(\varphi_0, \theta_0\right)$, $F_{r\varphi}\left(\varphi_0, \theta_0\right)$ and $F_{r\theta}\left(\varphi_0, \theta_0\right)$.

According to the angle measurement principle of radar. Sum channel signal S and the difference channel signal D_φ are represented as

$$S = E_1 + E_2 + E_3 + E_4 = 4F_r\left(e_1 + e_2 + e_3\right) \tag{22}$$

$$D_\varphi = E_2 + E_4 - E_1 - E_3 = 4F_{r\varphi}\left(\varphi_1' e_1 - \varphi_2' e_2 + \varphi_3' e_3\right) \tag{23}$$

The channel signal ratio is

$$M_\varphi = \Re\left(\frac{D_\varphi}{S}\right) = k_{r\varphi}\varphi + k_{r\varphi}\Re\left[\frac{\varphi_1 - \alpha\varphi_2 e^{j\delta_{12}} + \beta\varphi_3 e^{j\delta_{13}}}{1 + \alpha e^{j\delta_{12}} + \beta e^{j\delta_{13}}}\right] \tag{24}$$

where

$$\begin{cases} A_1' = A_1 F_j\left(\varphi_j - \varphi_1, \theta_j + \theta_1\right) \\ A_2' = A_2 F_j\left(\varphi_j + \varphi_2, \theta_j + \theta_2\right) \\ A_3' = A_3 F_j\left(\varphi_j - \varphi_3, \theta_j - \theta_3\right) \end{cases} \tag{25}$$

where $\Re$ stands for the real part.

$k_{r\varphi} = F_{r\varphi}\left(\varphi_0, \theta_0\right) / F_r\left(\varphi_0, \theta_0\right)$; $\alpha = A_2'/A_1'$ and $\beta = A_3'/A_1'$ are the jamming signal amplitude ratio of jamming antennas a_2 and a_3 to a_1. The formula of angle measurement is obtained as

$$\varphi_i = \frac{M_\varphi}{k_{r\varphi}} = \varphi + \Re\left(\frac{\varphi_1 - \alpha\varphi_2 e^{j\delta_{12}} + \beta\varphi_3 e^{j\delta_{13}}}{1 + \alpha e^{j\delta_{12}} + \beta e^{j\delta_{13}}}\right) \tag{26}$$

The first term in the above formula is the true target angle information. The second item is the angle measurement error introduced by jamming. It is obviously that the radar will obtain a wrong angle information, we can name this wrong angle "false target," it isn't means jamming result can generate an actual target but angle error to radar receiver. Equation (26) perfectly explains the generation of false targets. The second term can be controlled by adjusting the feed of jamming antenna then we can get the "false target" in anywhere position on a two-dimension plane. The conclusion is that the jamming method we proposed has a wider jamming range in space, which was obtained by comparing the proposed method other single-baseline jamming methods such as cross-eye jamming.

Using the second term of (26), the azimuth gain of the jamming antenna can be defined as:

$$G_\varphi = \Re\left(\frac{\varphi_1 - \alpha\varphi_2 e^{j\delta_{12}} + \beta\varphi_3 e^{j\delta_{13}}}{1 + \alpha e^{j\delta_{12}} + \beta e^{j\delta_{13}}}\right) \tag{27}$$

Similarly, the pitch angle gain of the jamming antenna can be obtained as follows:

$$G_\theta = \Re\left(\frac{\theta_1 + \alpha\theta_2 e^{j\delta_{12}} - \beta\theta_3 e^{j\delta_{13}}}{1 + \alpha e^{j\delta_{12}} + \beta e^{j\delta_{13}}}\right) \tag{28}$$

B. THE SECOND ERROR ANGLE DERIVATION METHOD, PHASE

The second method was the radar phase comparison method, as shown in Fig.3.

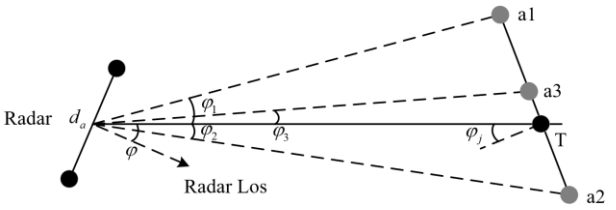

FIGURE 3. Schematic diagram of azimuth relationship between radar and three jamming antennas.

The most accurate angular relationship is shown in Fig.3. It is noted that the position of three antennas in second way is same as the first way, Fig.3 just shows that the angle relationship between radar and three jamming antennas. The second way was derived by using phase element, and the time harmonic function factor was replaced by phase factor phi. The specific derivation process will be described below.

The gain of radar sum channel in target T direction is expressed as [12]

$$S_0 = \cos\left[k\frac{d_a}{2}\sin\left(\varphi\right)\right] F_r\left(\varphi\right) \tag{29}$$

The coordinate of a_1, a_2, a_3 are $(\varphi_1, \theta_1), (\varphi_2, \theta_2), (\varphi_3, \theta_3)$. where k is the free-space phase constant, φ is the offset angle of target T from radar Los, φ_j is the jamming platform deflection angle, d_a is the spacing between the two antennas of radar, and $F_r(\varphi, \theta)$ is the Radar antenna beam function. The gains of the sum and difference channels in the three jamming antennas can be obtained as follows:

$$\begin{cases} \varphi_{a1} = \varphi + \varphi \\ \varphi_{a2} = \varphi - \varphi_2 \\ \varphi_{a3} = \varphi + \varphi_3 \end{cases} \tag{30}$$

$$S_i = \cos\left[k\frac{d_a}{2}\sin(\varphi_{ai})\right] F_r(\varphi_{ai})$$
$$D_i = j\sin\left[k\frac{d_a}{2}\sin(\varphi_{ai})\right] F_r(\varphi_{ai}) \tag{31}$$

where S_i and D_i $(i = 1, 2, 3)$ are represent the sum and difference channel gains in the direction of the nth jamming antenna, respectively.

Sum channel signal S and the difference channel D signal are represented as

$$S = S_0 \sum_{i=1}^{3} A_i S_i F_j(\varphi_{ai}) e^{j(\omega t + \delta 1 i)} \tag{32}$$

$$D = S_0 \sum_{i=1}^{3} A_i D_i F_j(\varphi_{ai}) e^{j(\omega t + \delta 1 i)} \tag{33}$$

$\delta_{1i}, (i = 1, 2, 3)$ is the phase difference of jamming antennas a_i relative to a_1. The channel signal ratio can be expressed as (34), shown at the bottom of the page, where $\Im$ denotes the imaginary part. We convert the imaginary part of the formula to the real part in this step. This is conducive to suture work. And there are

$$s_i = \cos\left[k\frac{d_a}{2}\sin(\varphi_{ai})\right], \quad d_i = \sin\left[k\frac{d_a}{2}\sin(\varphi_{ai})\right] \tag{35}$$

where $A_i' = A_i F_j(\varphi_{ai}), i = 1, 2, 3, \alpha = A_2'/A_1'$, and $\beta = A_3'/A_1'$ are the jamming signal amplitude ratios of the jamming antennas a_2 and a_3 to a_1; φ_1, φ_2, and φ_3 are very small when jamming is performed. Because the radar and jamming antenna are almost aligned, and the spacing of the jamming antenna is too small relative to the jamming distance, φ_1, φ_2, and φ_3 can be ignored. The radar antenna beam function is approximated as follows:

$$F_r(\varphi \pm \varphi_i) \approx F_r(\varphi) \tag{36}$$

where (34) can be obtained as follow

$$\tilde{M}_\varphi' = \Re\left(\frac{d_1 + \alpha d_2 e^{j\delta_{12}} + \beta d_3 e^{j\delta_{13}}}{s_1 + \alpha s_2 e^{j\delta_{12}} + \beta s_3 e^{j\delta_{13}}}\right) \tag{37}$$

To explain the derivation process more clearly, a detailed formula of the conversion process is given as (38), shown at the bottom of the page, where

$$m_i = k\frac{d_a}{2}\sin\varphi\cos\varphi_i, \quad n_i = k\frac{d_a}{2}\cos\varphi\sin\varphi_i, \ i = 1, 2, 3 \tag{39}$$

For the same reason, $\varphi_1, \varphi_2, \varphi_3$ is very small and can be ignored when jamming is applied. So

$$\lim_{\varphi_n \to 0}\cos(\varphi_n) = 1, \quad \lim_{\varphi_n \to 0}\sin(\varphi_n) = \varphi_n \tag{40}$$

Then (39) can be simplified like this.

$$m_i = k\frac{d_a}{2}\sin\varphi, \quad n_i = k\frac{d_a}{2}\varphi_i\cos\varphi, \quad i = 1, 2, 3 \tag{41}$$

Setting $m_i = m$, we will further derive formula (38) and replace the complex part with index (43). Result can be obtained as follow:

$$\tilde{M}_\varphi' = \Re\left[\frac{V\sin m + W\cos m}{V\cos m - W\sin m}\right] = \Re\left[K\left(\tan m + \frac{W}{V}\right)\right]$$
$$= \tan m \cdot \Re(K) + \Re\left(K \cdot \frac{W}{V}\right) \tag{42}$$

where V, W are indexes and can be written as

$$V = \cos n_1 + \alpha e^{\delta_{12}}\cos n_2 + \beta e^{\delta_{13}}\cos n_3$$
$$W = \sin n_1 - \alpha e^{\delta_{12}}\sin n_2 + \beta e^{\delta_{13}}\sin n_3 \tag{43}$$

$$\tilde{M}_\varphi' = \Im\left(\frac{D}{S}\right) = \Im\left[\frac{\sum_{i=1}^{3} A_i S_i F_j(\varphi_{ai}) e^{j(\omega t + \delta 1 i)}}{\sum_{i=1}^{3} A_i D_i F_j(\varphi_{ai}) e^{j(\omega t + \delta 1 i)}}\right]$$
$$= \Im\left[\frac{A_1' D_1 e^{j\omega t} + A_2' D_2 e^{j(\omega t + \delta_{12})} + A_3' D_3 e^{j(\omega t + \delta_{13})}}{A_1' S_1 e^{j\omega t} + A_2' S_2 e^{j(\omega t + \delta_{12})} + A_3' S_3 e^{j(\omega t + \delta_{13})}}\right]$$
$$= \Re\left[\frac{d_1 F_r(\varphi + \varphi_1) + \alpha d_2 F_r(\varphi - \varphi_2) e^{j\delta_{12}} + \beta d_3 F_r(\varphi + \varphi_3) e^{j\delta_{13}}}{s_1 F_r(\varphi + \varphi_1) + \alpha s_2 F_r(\varphi - \varphi_2) e^{j\delta_{12}} + \beta s_3 F_r(\varphi + \varphi_3) e^{j\delta_{13}}}\right] \tag{34}$$

$$\tilde{M}_\varphi' = \Re\left[\frac{\sin(m_1 + n_1) + \alpha\sin(m_2 - n_2) e^{j\delta_{12}} + \beta\sin(m_3 + n_3) e^{j\delta_{13}}}{\cos(m_1 + n_1) + \alpha\cos(m_2 - n_2) e^{j\delta_{12}} + \beta\cos(m_3 + n_3) e^{j\delta_{13}}}\right] \tag{38}$$

Index K was used in the simplification of (42). There are

$$K = \frac{V \cdot \cos m}{V \cdot \cos m - W \cdot \sin m} \tag{44}$$

Radar and jamming antennas will be almost aligned when the jamming antennas begin to implement jamming, which makes φ become small and $K \approx 1$, φ can be ignored in the process of derivation. We continue to deduce formula (42) in conjunction with index (43). The following results were obtained.

$$\begin{aligned}\tilde{M}'_{\varphi} &= \tan m + \Re\left(\frac{W}{V}\right) \\ &= \tan m + \Re\left(\frac{\sin n_1 - \alpha e^{\delta_{12}} \sin n_2 + \beta e^{\delta_{13}} \sin n_3}{\cos n_1 + \alpha e^{\delta_{12}} \cos n_2 + \beta e^{\delta_{13}} \cos n_3}\right)\end{aligned} \tag{45}$$

It is obvious that formula (45) includes the feed parameter of jamming antennas, which means the received signals $\tilde{M}'_{\varphi}$ including the jamming information.

When jamming does not exist, the result can be obtained by deriving (29) in the same way from (30) to (34). According to the received echo, the channel signal ratio without jamming generated by the radar can be expressed as

$$\begin{aligned}M'_{\varphi} &= \Im\left(\frac{S_0 D_0}{S_0 S_0}\right) \\ &= \Im\left\{\frac{j \sin\left[k\frac{d_a}{2}\sin(\varphi)\right] F_r(\varphi)}{\cos\left[k\frac{d_a}{2}\sin(\varphi)\right] F_r(\varphi)}\right\} = \tan\left[k\frac{d_a}{2}\sin(\varphi)\right]\end{aligned} \tag{46}$$

The jamming antenna starts jamming only when the detection radar continuously transmits the detection signal and is approaching or already approaching jamming platform, φ and θ is very small when interference is applied. Because the jamming distance is far greater than the distance between the jamming antenna and center T, $m_1, n_1, m_2, n_2, m_3, n_3$ is very small. Refer to "(40)," we can facilitate the formula (45) and (46) like this.

$$M'_{\varphi} = \tan\left[k\frac{d_a}{2}\sin(\varphi)\right] \approx k\frac{d_a}{2}\sin(\varphi) \tag{47}$$

$$\begin{aligned}\tilde{M}'_{\varphi} &= \tan m + \Re\left(\frac{\sin n_1 - \alpha e^{\delta_{12}} \sin n_2 + \beta e^{\delta_{13}} \sin n_3}{\cos n_1 + \alpha e^{\delta_{12}} \cos n_2 + \beta e^{\delta_{13}} \cos n_3}\right) \\ &= \tan m + \Re\left(\frac{n_1 - \alpha n_2 e^{j\delta_{12}} + \beta n_3 e^{j\delta_{13}}}{1 + \alpha e^{j\delta_{12}} + \beta e^{j\delta_{13}}}\right) \\ &= k\frac{d_a}{2}\sin(\varphi) + \Re\left(\frac{\varphi_1 - \alpha\varphi_2 e^{j\delta_{12}} + \beta\varphi_3 e^{j\delta_{13}}}{1 + \alpha e^{j\delta_{12}} + \beta e^{j\delta_{13}}}\right)\end{aligned} \tag{48}$$

The expression error angle gain can be obtained by combining equations (47) and (48), one of which includes the jamming angle information, and the other is the angle information without jamming. The second complex expression term in (48) is introduced by the jamming antennas.

Then the error angle gain formula can be obtained as follow

$$G_{\varphi} = \Re\left(\frac{\varphi_1 - \alpha\varphi_2 e^{j\delta_{12}} + \beta\varphi_3 e^{j\delta_{13}}}{1 + \alpha e^{j\delta_{12}} + \beta e^{j\delta_{13}}}\right) \tag{49}$$

Similarly, the pitch angle gain of the jamming antenna can be obtained. The error angle gain formula expresses the error term of the angle measurement. Finally, the error angle formulas for two measurement methods were compared. It is found that the result of angle measurement error gain of two methods is the same, refer to "(27) and (49)." The mathematical model verifies the feasibility of the multiple-antenna synthetic jamming method.

IV. PHASE PARAMETER TOLERANCE ANALYSIS

A. CROSS-EYE JAMMING

W. P. du Plessis analyzed the phase comparison radar sum and difference echo signals. A rigorous mathematical model for inverse cross-eye interference is derived. The cross-eye gain is defined as follows [12].

$$G_C = \frac{1 - \alpha^2}{1 + \alpha^2 + 2\alpha\cos\delta} \tag{50}$$

This is shown in the Fig.4(a). When the phase difference between the two antennas is 180° the amplitude ratio between the two jamming antennas is 0dB. The absolute value of the cross-eye gain reaches infinity (to ensure the visibility of the image, only finite value of the cross-eye gain is given). This is the reason why cross-eye jamming requires two jamming antennas to have equal amplitude and a 180° phase difference.

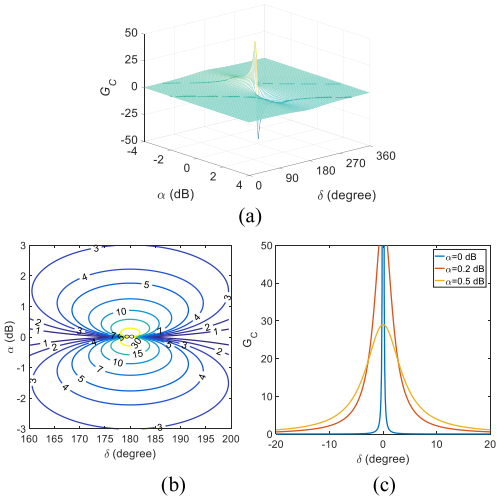

FIGURE 4. Relationship between cross-eye gain and amplitude ratio and phase difference of jamming antenna (a). Cross-eye gain tolerance contour map (b). Phase diagram tolerance of cross-eye gain when amplitude ratio is 0dB, 0.2dB and 0.5dB respectively (c).

This can be concluded from Figs.4(b) and (c). The cross-eye gain decreases sharply when the parameter (α, δ) deviates from the extreme point $(0\text{dB}, 180°)$. This shows that the cross-eye gain is very strict for the feed-parameter tolerance of the jamming antenna. As shown in the figure above, a contour map of the absolute value of the cross-eye gain within a certain parameter tolerance is provided. This part of the diagram was used for the subsequent comparisons.

TABLE 1. The feeding parameters of jamming antenna and the maximum value of the synthrtic gain of three antennas.

Gain	Maximum value	α	β	δ_{12}	δ_{13}
G_φ	$+\infty$ / $-\infty$	0 dB	0 dB	120°	240°
	$+\infty$ / $-\infty$	0 dB	0 dB	240°	120°
G_θ	$+\infty$ / $-\infty$	0 dB	0 dB	120°	240°
	$+\infty$ / $-\infty$	0 dB	0 dB	240°	120°

B. MULTIPLE ANTENNAS SYNTHETIC FALSE TARGET JAMMING

The formula and mechanism of synthetic false target interference from multiple antennas have been studied extensively in this chapter. We can conclude that the larger the combined gain of three antennas, the larger is the angle measurement error. Therefore, it is necessary to solve the feed parameter results of the jamming antennas to maximize the combined gain of the three antennas.

To investigate what kind of parameters that affect the value of G_φ, it is necessary to expand its expression of G_φ.The derived jamming gain expressions (27) and (28) can be expanded as follows (only the expression of G_φ has been proposed to make the article more concise, because G_θ and G_φ are similar)

$$\begin{aligned} G_\varphi = & [\varphi_1 - \alpha^2\varphi_2 + \beta^2\varphi_3 + \alpha(\varphi_1 - \varphi_2)\cos\delta_{12} \\ & + \beta(\varphi_1 + \varphi_3)\cos\delta_{13} + \alpha\beta(\varphi_3 - \varphi_2)\cos(\delta_{12} - \delta_{13})] \\ & \div [1 + \alpha^2 + \beta^2 + 2\alpha\cos\delta_{12} + 2\beta\cos\delta_{13} \\ & + 2\alpha\beta\cos(\delta_{12} - \delta_{13})] \end{aligned} \tag{51}$$

Equation (51) shows that the amplitude ratio, phase difference, and coordinates of the three jamming antennas can significantly influence the gain value. All factors affecting the jamming gain will be investigated. First, we defined the coordinates of the three antennas as follows: a_1, a_2, a_3 (−15m, 0m, 0m), (15m, 0m, 0m) and (0m, 13m, 0m). The given coordinates are not a special situation in this example; they can be given casually whether it is an equilateral triangle or an isosceles triangle. Letting the r equal 1000(units of meters), the result can be obtained as

$$\begin{cases} \varphi_1 = 0.015 \text{ rad}, & \theta_1 = 0.000 \text{ rad} \\ \varphi_2 = 0.015 \text{ rad}, & \theta_2 = 0.000 \text{ rad} \\ \varphi_3 = 0.000 \text{ rad}, & \theta_3 = 0.013 \text{ rad} \end{cases} \tag{52}$$

Combining the above values (52) and formula (51), the calculation results are obtained and shown in the table below (To facilitate the calculation and analysis process, the antenna coordinates are initially assigned according to the existing simple model. More accurate coordinates of the jamming antenna are determined by the model of the catual carrier).

The gain of the multi-antenna interference is maximized only when the data meet the conditions in the table above. The concept of angle factor (AF) was introduced. The angle factor AF is defined as the absolute value of the ratio of the combined gain of the three antennas to the maximum angle of the jamming antenna. AF_φ is the azimuth gain angle factor, AF_θ is the pitch angle gain angle factor, and AF_T is the total gain angle factor of the three antennas. The expression is as follows:

$$\begin{cases} AF_\varphi = \left| \dfrac{G_\varphi}{\max(\varphi_i)} \right|, & AF_\theta = \left| \dfrac{G_\theta}{\max(\theta_i)} \right| \\ AF_T = \left| \dfrac{G_{\text{total}}}{\max(\varphi_i, \theta_i)} \right|, & (i = 1, 2, 3) \end{cases} \tag{53}$$

The same principle defines the angle factor of the cross-eye jamming gain AF_C. When the angle factor AF is greater than 1, it means that the position of the false target is apparently outside the jamming system carrier. The significance of parameter tolerance analysis is in obtaining the angle factor that ensures that the carrier is not detected by radar, and the allowable error range of the jamming antenna feed parameters is given below. There are two groups of the jamming antenna feed parameters (α, δ_{12}) and (β, δ_{13}),and, when the plane angle of the jamming antenna is $\varphi_j = 0, \theta_j = 0$. Setting $\beta = 0, \delta_{13} = 240°$,the contour map of AF_φ and AF_θ are given in the Fig.5 (In order to ensure the refinement of this article, only the results under the above limited conditions are provided, which does not mean that a good conclusion can be drawn only under these conditions. This method had a stable tolerance range under all limiting conditions).

Because the parameters were set at the beginning of the calculation, the azimuth angles of the three antennas were set to be larger. Comparing the results of the contour maps in Fig.5, it can be concluded that AF_φ has a wider phase parameter tolerance than AF_θ because the jamming antenna coordinates in azimuth are wider, it can be seen from the calculation results of equation (52). Although AF_T and AF_C has the same parameter tolerance range in the below figures. It's worth noting that three antennas synthetic jamming has a wider phase parameter tolerance when the amplitude ratio α is close to the ideal value of 0dB. This is the superiority of the jamming method proposed in this paper. There will be more specific explanations later.

In practice, the actual feed parameters obtained by the interfering antenna are unlikely to be theoretical feed values. We know that the inaccuracy of feeding cannot guarantee a very accurate amplitude ratio relationship between jamming antennas owing to the assembly of mechanical devices and the influencing factors of the external field environment. Thus, it is necessary to conduct a parameter tolerance analysis for the jamming method. As shown in the Fig.6. Both AF_C and AF_T have good phase tolerance results at $\alpha = 0.5dB$. The tolerance of the phase-difference parameter AF_C is get smaller, when the amplitude ratio α is closer to the ideal value of 0dB. A small phase error results a sharp decline in the interference gain of the cross-eye jamming method. AF_C will be below 1 or even 0 when $\alpha = 0$ dB especially. On the contrary, the phase error tolerance of the three antennas synthetic false target jamming is always stable at $\pm 10°$ above when AF_T equals 5, which means that the angle error caused by

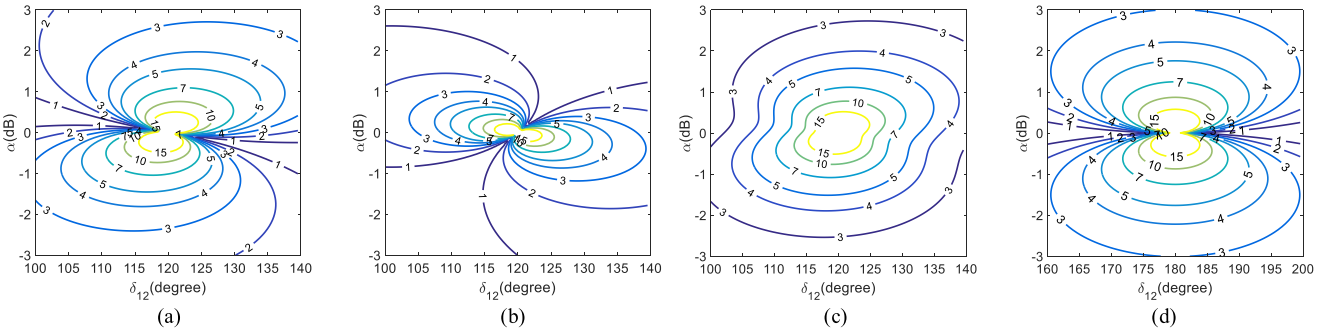

FIGURE 5. Parameter tolerance contour map of AF_{φ} (a) AF_{θ} (b) AF_{T} (c), and AF_{C} (d).

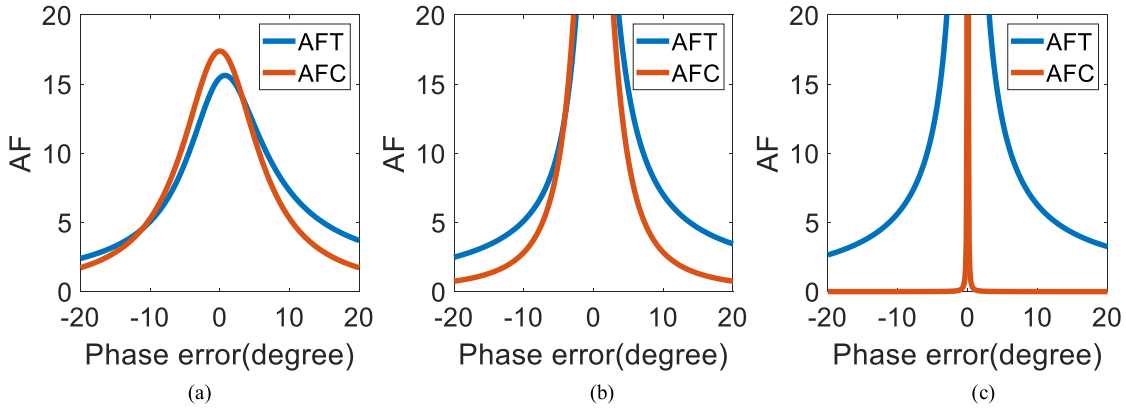

FIGURE 6. Tolerance of phase difference parameters with the same amplitude ratio; (a) $\alpha = 0.5$dB; (b) $\alpha = 0.2$dB; (c) $\alpha = 0$dB.

the jamming system is very large, and the false target will fall approximately five times farther from the carrier than the maximum spacing of the jamming antennas. Thus, it can be seen that the three antennas synthetic false target jamming has a higher phase-difference tolerance than the cross-eye jamming method under the same mathematical conditions. A wider parameter tolerance means that the jamming method proposed in this paper has a higher possibility and a more stable interference effect in real applications. Even if it is affected by many factors, the jamming antenna cannot obtain an accurate feed, and the method we proposed in this paper can still complete the interference owing to the wide phase parameter tolerance, which is the advantage of the method proposed in this paper.

V. CONCLUSION

The main contribution of this study is a new jamming method for angle measurement errors that has a wider phase parameter tolerance to ensure successful jamming with a high probability in practical applications. The main objective of this study is to establish a strict scientific mathematical model for a multiple antennas synthetic false target jamming scene and derive a mathematical formula for the jamming error angle. The following results were derived for the multiple antennas synthetic false target jamming, the angle measurement error formula of two different methods under three antennas synthetic jamming is obtained; The gain of jamming antenna in azimuth and pitch angle is obtained. We can see that multiple-antenna synthetic false target jamming can effectively jam radar with two different angle-measurement methods by comparing the error angle gain formula with two different angle-measurement methods. It can be found that the jamming method proposed in this paper has two-dimensional plane jamming range by observing the result of mathematical derivation. Overall, the jamming method proposed in this study has two advantages. First the range of interference was wider. The ''false target'' can be obtained on two-dimensional plane rather than on the one-dimensional range, the other one is that the phase parameter tolerance of multiple antennas synthetic false target jamming is broader than that of cross-eye jamming intuitively. The advantages and reliability of the proposed jamming method are visualized by charts, contour maps, and three-dimensional curves in this study through the establishment, derivation, calculation, and analysis of the multiple antennas synthetic false target jamming model. The final result shows that the multiple-antenna synthetic false target jamming proposed in this paper makes the jamming range wider and more stable.

REFERENCES

[1] P. Redmill, *The Principles of Artifical Glint Jamming (Cross Eye)*, 1963, p. 47.
[2] W. J. Kerins, ''Analysis of towed decoys,'' *IEEE Trans. Aerosp. Electron. Syst.*, vol. 29, no. 4, pp. 1222–1227, Oct. 1993.

[3] L. Falk, "Cross-eye jamming of monopulse radar," in *Proc. Int. Waveform Diversity Design Conf.*, Jun. 2007, pp. 209–213.
[4] F. Neri, "Anti-monopulse jamming techniques," in *IEEE MTT-S Int. Microw. Symp. Dig.*, Aug. 2001, pp. 45–50.
[5] W. P. duPlessis, J. W. Odendaal, and J. Joubert, "Experimental simulation of retrodirective cross-eye jamming," *IEEE Trans. Aerosp. Electron. Syst.*, vol. 47, no. 1, pp. 734–740, Jan. 2011.
[6] S. Y. Liu, C. X. Dong, J. Xu, G. Q. Zhao, and Y. T. Zhu, "Analysis of rotating cross-eye jamming," *IEEE Antennas Wireless Propag. Lett.*, vol. 14, pp. 939–942, 2015.
[7] T. Liu, D. Liao, X. Wei, and L. Li, "Performance analysis of multiple-element retrodirective cross-eye jamming based on linear array," *IEEE Trans. Aerosp. Electron. Syst.*, vol. 51, no. 3, pp. 1867–1876, Jul. 2015.
[8] W. P. du Plessis, "Cross-eye gain in multiloop retrodirective cross-eye jamming," in *Proc. 12th Int. Conf. Signal Process. (ICSP)*, May 2014, pp. 2135–2140.
[9] W. D. Plessis, "Cross-eye gain in multiloop retrodirective cross-eye jamming," *IEEE Trans. Aerosp. Electron. Syst.*, vol. 52, no. 2, pp. 875–882, Apr. 2016.
[10] W. P. Du Plessis, "Platform skin return and retrodirective cross-eye jamming," *IEEE Trans. Aerosp. Electron. Syst.*, vol. 48, no. 1, pp. 490–501, Jan. 2012.
[11] W. P. duPlessis, J. W. Odendaal, and J. Joubert, "Tolerance analysis of cross-eye jamming systems," *IEEE Trans. Aerosp. Electron. Syst.*, vol. 47, no. 1, pp. 740–745, Jan. 2011.
[12] W. P. du Plessis, *A Comprehensive Investigation of Retrodirective Cross-Eye Jamming*. Pretoria, South Africa: Univ. Pretoria, 2010, pp. 38–42.
[13] W. P. du Plessis, "Path-length effects in multiloop retrodirective cross-eye jamming," *IEEE Antennas Wireless Propag. Lett.*, vol. 15, pp. 626–629, 2016, doi: 10.1109/LAWP.2015.2465815.
[14] W. P. du Plessis, "Analysis of path-length effects in multiloop cross-eye jamming," *IEEE Trans. Aerosp. Electron. Syst.*, vol. 53, no. 5, pp. 2266–2276, Oct. 2017, doi: 10.1109/TAES.2017.2690538.
[15] W. P. D. Plessis, "Path-length compensation in multiloop retrodirective cross-eye jamming," *IEEE Trans. Aerosp. Electron. Syst.*, vol. 55, no. 1, pp. 397–406, Feb. 2019, doi: 10.1109/TAES.2018.2852378.
[16] W. P. Plessis, "Phase-conjugating retrodirective cross-eye jamming," *Electron. Lett.*, vol. 56, no. 20, pp. 1079–1082, Sep. 2020.
[17] W. Liu, J. Meng, and L. Zhou, "Method of four-element retrodirective cross-eye jamming based on DoA," *IEEE Access*, vol. 8, pp. 76896–76902, 2020, doi: 10.1109/ACCESS.2020.2990906.
[18] I. S. Kim, J. Park, G. Kim, B. Park, and Y. Jang, "Study on retrodirective cross-eye structure using linear phased array antenna," *J. Korea Inst. Mil. Sci. Technol.*, vol. 23, no. 1, pp. 11–17, 2020.
[19] F. Pieterse and W. P. du Plessis, "Retrodirective cross-eye jammer implementation using software-defined radio (SDR)," in *Proc. IEEE Radar Conf. (RadarConf)*, May 2021, pp. 1–4, doi: 10.1109/RadarConf2147009.2021.9455215.
[20] G. W. Lank and G. E. Pollon, "Exact angular accuracy of an amplitude comparison sequential-lobing processor," *IEEE Trans. Aerosp. Electron. Syst.*, vol. AES-10, no. 3, pp. 393–398, May 1974, doi: 10.1109/TAES.1974.307950.
[21] W. P. du Plessis, J. W. Odendaal, and J. Joubert, "Extended analysis of retrodirective cross-eye jamming," *IEEE Trans. Antennas Propag.*, vol. 57, no. 9, pp. 2803–2806, Sep. 2009, doi: 10.1109/TAP.2009.2027353.
[22] D. Barton and S. Sherman, *Monopulse Principles and Techniques*, 2nd ed. Norwood, MA, USA: Artech House, 2011.

YUHANG NING was born in Xi'an, Shaanxi, China, in 1998. He is currently pursuing the master's degree with the School of Physics, University of Electronic Science and Technology of China. His research interests include radar electromagnetic jamming and microwave and millimeter wave circuits and systems.

MENGXIA YU received the master's and Ph.D. degrees in engineering from the University of Electronic Science and Technology of China, Chengdu, China, in 1997 and 2005, respectively. She was a Visiting Scholar at the University of California, San Francisco, from 2010 to 2011. She is currently a Researcher with the School of Physics, University of Electronic Science and Technology of China. She has authored or coauthored over 20 papers in her research fields. Her research interests include radar electromagnetic jamming, microwave circuits and systems, circuit devices, system in package circuits, bioelectromagnetic effects, and terahertz circuits and systems.